ACCOUNTS
of chemical research

Phosphate Binding Energy and Catalysis by Small and Large Molecules

JANET R. MORROW, TINA L. AMYES, AND JOHN P. RICHARD*
Department of Chemistry, University at Buffalo, State University of New York, Buffalo, New York 14260-3000

RECEIVED ON SEPTEMBER 11, 2007

CONSPECTUS

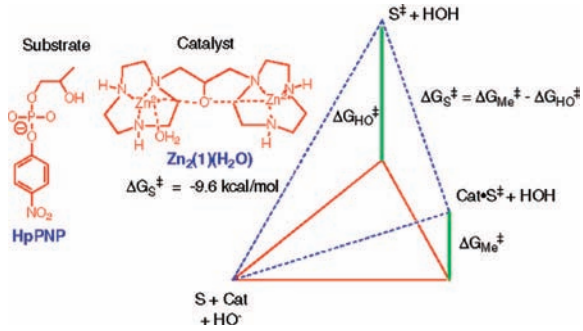

Catalysis is an important process in chemistry and enzymology. The rate acceleration for any catalyzed reaction is the difference between the activation barriers for the uncatalyzed ($\Delta G_{HO}^{\ddagger}$) and catalyzed ($\Delta G_{Me}^{\ddagger}$) reactions, which corresponds to the binding energy ($\Delta G_S^{\ddagger} = \Delta G_{Me}^{\ddagger} - \Delta G_{HO}^{\ddagger}$) for transfer of the reaction transition state from solution to the catalyst. This transition state binding energy is a fundamental descriptor of catalyzed reactions, and its evaluation is necessary for an understanding of any and all catalytic processes. We have evaluated the transition state binding energies obtained from interactions between low molecular weight metal ion complexes or high molecular weight protein catalysts and the phosphate group of bound substrate. Work on catalysis by small molecules is exemplified by studies on the mechanism of action of Zn_2(**1**)(H_2O). A binding energy of $\Delta G_S^{\ddagger} = -9.6$ kcal/mol was determined for Zn_2(**1**)(H_2O)-catalyzed cleavage of the RNA analogue HpPNP. The pH−rate profile for this cleavage reaction showed that there is optimal catalytic activity at high pH, where the catalyst is in the basic form [Zn_2(**1**)(HO^-)]. However, it was also shown that the active form of the catalyst is Zn_2(**1**)(H_2O) and that this recognizes the C2-oxygen-ionized substrate in the cleavage reaction. The active catalyst Zn_2(**1**)(H_2O) shows a high affinity for oxyphosphorane transition state dianions and a stable methyl phosphate transition state analogue, compared with the affinity for phosphate monoanion substrates. The transition state binding energies, $\Delta G_S^{\ddagger}$, for cleavage of HpPNP catalyzed by a variety of Zn^{2+} and Eu^{3+} metal ion complexes reflect the increase in the catalytic activity with increasing total positive charge at the catalyst. These values of $\Delta G_S^{\ddagger}$ are affected by interactions between the metal ion and its ligands, but these effects are small in comparison with $\Delta G_S^{\ddagger}$ observed for catalysis by free metal ions, where the ligands are water. Enzymes are unique in having evolved mechanisms to effectively utilize binding interactions with nonreacting fragments of the substrate in stabilization of the reaction transition state. Orotidine 5′-monophosphate decarboxylase, α-glycerol phosphate dehydrogenase, and triosephosphate isomerase catalyze dissimilar decarboxylation, hydride transfer, and proton transfer reactions, respectively. Each enzyme derives ca. 12 kcal/mol of transition state stabilization from protein interactions with the nonreacting phosphate group, which is larger than the highest ~10 kcal/mol transition state stabilization that we have determined for small-molecule catalysis of phosphate diester cleavage in water. Each of these enzymes catalyze the slow reaction of a truncated substrate that lacks the phosphate group, and in each case, the reaction of the truncated substrate is strongly activated by the *allosteric* binding of the second substrate "piece" phosphite dianion, HPO_3^{2-}. We propose a modular design for these enzymes with a classical active site that recognizes the reactive substrate fragment and a separate phosphodianion binding site. The second site is created, in part, by flexible protein loops that wrap around the substrate phosphodianion group and *bury* the substrate in an environment with an optimal local dielectric constant for the catalyzed reaction and with the most favorable positioning of the catalytic side chains. This design is easily generalized to a wide variety of enzyme-catalyzed reactions.

Published on the Web 02/23/2008 www.pubs.acs.org/acr
10.1021/ar7002013 CCC: $40.75

Introduction

Linus Pauling noted that catalysis in general, and by enzymes in particular, will result from the development of tight interactions between the catalyst and the transition state for the catalyzed reaction.[1] This is shown by the transition state binding energy, $\Delta G_S^{\ddagger}$ (Scheme 1). Catalysis by most enzymes is so efficient that release of products would be strongly rate-determining if they were to bind with the same affinity as the transition state. Consequently, enzymes show a large discrimination and bind their substrates/products much more weakly than the reaction transition state (Scheme 1).[2]

The Pauling paradigm has a particular appeal when trying to explain catalysis to students. On the other hand, there are issues that must be addressed if this model is to be accepted as a starting framework for explaining enzyme catalysis. These include the following:

(1) Recently, Zhang and Houk wrote: "While complementarity of the type proposed by Pauling can account for acceleration up to 11 orders of magnitude, most enzymes exceed that proficiency."[3] They therefore proposed that enzymes "achieve over 15 kcal/mol of *transition state binding* not merely by a concatenation of noncovalent effects but by covalent bond formation between enzyme or cofactor and transition state, involving a change in mechanism from that in aqueous solution."[3]

(2) There are only small differences in the structure of the substrate/product and the transition state for many enzyme-catalyzed reactions. The origin of the large differential binding of these species is generally unknown.[2]

(3) Enzymes are large molecules that undergo many types of motion, some of which may be coupled to catalysis. Further, catalysis of chemical reactions must ultimately be explained at the level of quantum mechanics. Since neither protein dynamics nor quantum mechanics are central to the Pauling paradigm, more sophisticated models for catalysis might either use this paradigm as a starting point or as a specialized example or, in the most extreme case, discard it entirely.

Our goal as experimentalists has been to characterize the mechanisms for catalysis by small metal ion complexes and by larger enzymes where much or all of the catalytic power is derived from the utilization of phosphate binding energy. We summarize here the results of this work and provide an interpretation of our results within the framework of the Pauling model.

SCHEME 1

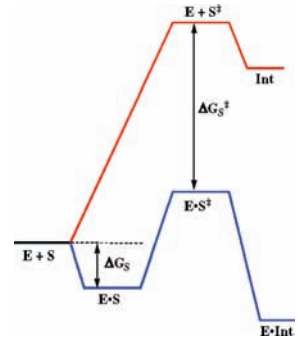

Phosphate Diester Cleavage

The design of catalysts to cleave RNA has considerable intellectual appeal, along with potential to produce RNA cleavage reagents that have practical applications.[4–6] J. R. Morrow and co-workers have shown that lanthanide(III) complexes are efficient catalysts of the cleavage of RNA,[7,8] and they have examined cleavage of the 5′ cap of mRNA by several metal ion−macrocycle complexes.[9] Recent collaborative work between the Morrow and Richard laboratories has focused on characterizing the rate acceleration for catalysis by metal ion complexes and defining the origin of the catalytic rate acceleration.

Kinetic Analyses. An examination of the literature suggested to us that the laboratory time expended in the synthesis of novel metal ion catalysts of RNA cleavage often exceeded the time spent in characterizing their kinetics and mechanism of action. In particular, it is difficult to compare the catalytic activity of metal ion complexes prepared in different laboratories, because there is no commonly agreed upon protocol for measuring and reporting the kinetic parameters for catalysis. Our initial goal was to develop such a protocol for reporting kinetic data for metal ion complex-catalyzed phosphate diester cleavage in water at 25 °C, in the hope that it might be adopted by other laboratories.

We have reported second-order rate constants k_{Me} for the catalyzed cleavage of HpPNP, UpPNP, and UpU to form cyclic

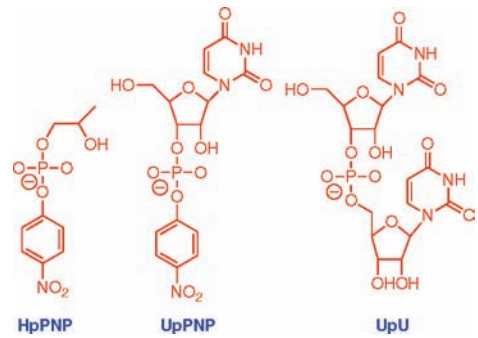

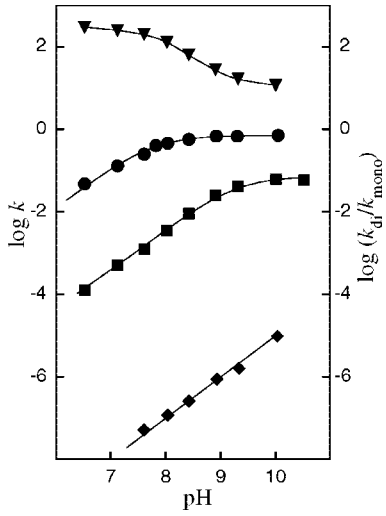

FIGURE 1. pH−rate profiles for cleavage of HpPNP catalyzed by HO^- and Zn(II) complexes in water at 25 °C:[10] (◆) k_{obsd} (s^{-1}) for spontaneous HO^--catalyzed cleavage; (■), k_{Me} (M^{-1} s^{-1}) for cleavage catalyzed by Zn(**2**)(H_2O); (●), k_{Me} (M^{-1} s^{-1}) for cleavage catalyzed by Zn_2(**1**)(H_2O); (▼), ratio of k_{Me} for cleavage catalyzed by the dinuclear (k_{di}) and mononuclear (k_{mono}) Zn(II) complexes.

phosphate diesters. These rate constants are generally determined as the slopes of linear plots of k_{obsd} (s^{-1}) for phosphate diester cleavage against the catalyst concentration. The rate constant k_{Me} has the same units (M^{-1} s^{-1}) and meaning as k_{cat}/K_m for an enzyme-catalyzed reaction. Values of k_{Me} determined at Buffalo and elsewhere can be directly compared in order to provide a simple and meaningful measure of the catalytic activity of different metal ion complexes or of their activity relative to enzyme catalysts.

The catalytic effectiveness of a variety of metal ion complexes was then evaluated over a broad range of pH. Figure 1 shows representative pH−rate profiles for the Zn_2(**1**)(H_2O)- and Zn(**2**)H_2O-catalyzed cleavage of HpPNP and for the spon-

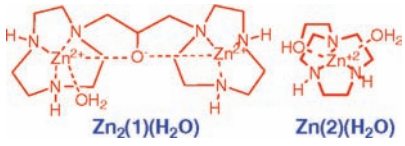

SCHEME 2

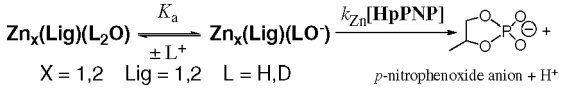

taneous specific-base-catalyzed cleavage of HpPNP.[10] These profiles show that the *complex* between HpPNP and the fully protonated catalyst is inactive and that this complex is converted to the active form upon loss of a proton. Maximal activity is observed at high pH, where the metal-bound water of the free catalyst is ionized. The pH− and pD−rate profiles for catalysis of the cleavage of HpPNP, UpPNP, and UpU by a broad range of mono- and dinuclear catalysts are also governed by ionization of a metal-bound water, as shown in Scheme 2.[10−19] The data in Figure 1 and that for related catalyzed reactions show a good fit to eq 1 derived for Scheme 2, which gave values of K_a similar to those determined by potentiometric titration.[10]

$$k_{Me} = \left[\frac{k_{Zn}K_a}{K_a + [H^+]}\right] \quad (1)$$

Figure 1 shows that the relative activity of Zn_2(**1**)(H_2O) and Zn(**2**)(H_2O) as catalysts of the cleavage of HpPNP depends upon whether the observed second-order rate constants k_{Me} are compared at high or low pH. There is only a 12-fold difference in the *apparent* reactivity of the dinuclear complex and the mononuclear complex at high pH. This difference increases to 290-fold for reactions at low pH because the downward break in catalytic activity is observed at a higher pH for Zn(**2**)(H_2O), as a result of the 1.2 unit higher pK_a for ionization of the zinc-bound water at Zn(**2**)(H_2O) than of that at Zn_2(**1**)(H_2O).[10]

The high catalytic activity of Zn_2(**1**)(H_2O) is notable because tethering two mononuclear Zn^{2+} complexes to form a dinuclear complex often causes only a statistical ca. 2-fold increase in catalytic activity.[15] The X-ray structure of crystals (grown at pH 6.0) of the perchlorate salt of Zn_2(**1**)(H_2O) shows that the two Zn^{2+} are separated by only 3.66 Å, due to shielding of the electrostatic interaction between the metal cations by the bridging alkoxide.[10] The interactions between the two Zn^{2+} and the linker alkoxide anion draw the metal cations into a densely charged core, which provides a particularly large electrostatic stabilization of the dianionic transition state for phosphate diester cleavage.[10,15]

Transition State Binding Energies

Our next goal was to obtain a simple measure of catalytic effectiveness from our kinetic data. The rate accelerations for the catalyzed cleavage of HpPNP, given by eq 2 derived for Scheme 3, were calculated from the relative displacement of the parallel lines for the formally HO^--catalyzed cleavage (◆, Figure 1) and the HO^--dependent metal ion complex catalyzed reactions (● and ■), where K_a is the ionization constant for the metal-bound water and $K_w = 10^{-14}$ M^2.[20] The transition state binding energies of $\Delta G_S^{\ddagger} = -9.6$ and -5.9 kcal/mol for the reactions catalyzed by Zn_2(**1**)(H_2O) ($K_a = 10^{-7.8}$ M) and Zn(**2**)(H_2O) ($K_a = 10^{-9.2}$ M) respectively, correspond to (1.1×10^7)-fold and (2.2×10^4)-fold rate accelerations over the specific-base-catalyzed reaction.[18,20] Zn_2(**1**)(H_2O) is an extremely impressive small

SCHEME 3

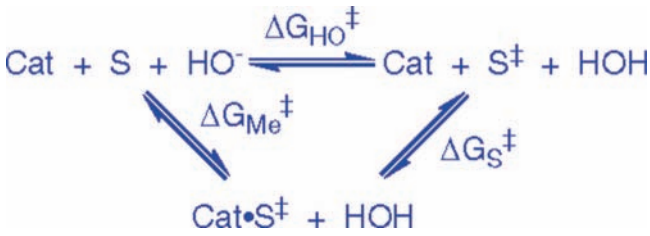

molecule catalyst. Metal ion complexes with even higher catalytic activity in water[21] and in methanol[22] have been prepared.

$$\Delta G_S^{\ddagger} = \Delta G_{Me}^{\ddagger} - \Delta G_{HO}^{\ddagger} = -RT\ln\left[\frac{k_{Zn}K_a/K_w}{k_{HO}}\right] \qquad (2)$$

Figure 2 shows the transition state binding energy as the difference in the activation barrier for HO^--catalyzed cleavage of an RNA analogue and for the metal ion complex-catalyzed reaction, which is also an HO^--dependent reaction (eq 2). The calculation of $\Delta G_S^{\ddagger}$ compresses extensive kinetic data into a single parameter that provides a direct measure for catalytic activity at neutral pH, where the catalyst is largely protonated. We have determined the values of $\Delta G_S^{\ddagger}$ for a wide variety of metal ion complex-catalyzed reactions and used these data to evaluate the effect of changing catalyst and substrate structure on catalytic activity.[11,14,16,18–20]

Active Form of Catalyst

The pH dependence (Figure 1) of the uncatalyzed and catalyzed cleavage of HpPNP at pH less than the catalyst pK_a shows that under these conditions a proton is lost from the catalyst or substrate on proceeding to the rate-determining transition state. This kinetic analysis cannot distinguish between (a) the loss of proton from the substrate, in which case Zn_2(**1**)(H_2O) is the active catalyst and (b) the loss of a proton from the catalyst, in which case the active form of the catalyst is Zn_2(**1**)(HO^-), whose concentration approaches a limit at pH > pK_a (Scheme 2).[10,12]

Analysis of inhibition of the Zn_2(**1**)(H_2O)-catalyzed cleavage of HpPNP shows that methylphosphate dianion binds to Zn_2(**1**)(H_2O) with a 1600-fold higher affinity than does diethylphosphate monoanion.[23] This strong and specific binding of the stable dianion resembles the specific binding of the dianionic transition state for cleavage of HpPNP to Zn_2(**1**)(H_2O), with an affinity that is much greater than that of the substrate monoanion.[10] We concluded that methyl phosphate dianion is a transition state analogue for the Zn_2(**1**)(H_2O)-catalyzed cleavage of phosphate diesters.[24]

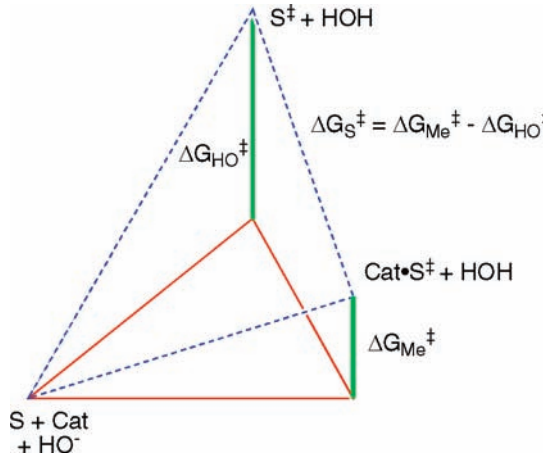

FIGURE 2. Bar graph that shows the barrier for HO^--promoted phosphate diester cleavage in water ($\Delta G_{HO}^{\ddagger}$, green bar), the barrier for the metal ion complex-catalyzed hydroxide ion-promoted reaction ($\Delta G_{Me}^{\ddagger}$, green bar), and the binding energy for the transition state for the aqueous HO^--promoted reaction ($\Delta G_S^{\ddagger}$).

SCHEME 4

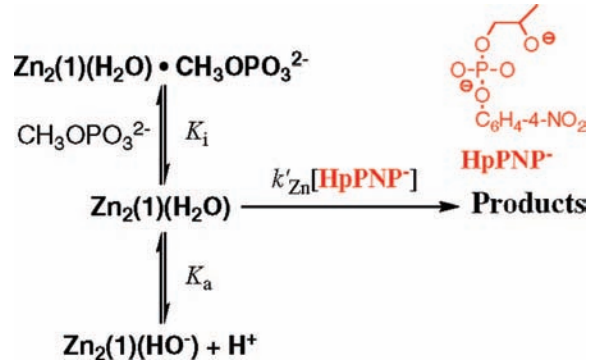

Apparent inhibition constants, K_i, for inhibition of Zn_2(**1**)(H_2O)-catalyzed cleavage of HpPNP by methyl phosphate dianion approach a limiting small value of 6×10^{-6} M for formation of a tight complex at low pH, where the catalyst exists mainly in the protonated form Zn_2(**1**)(H_2O).[23] These data (not shown) were fit to the model in Scheme 4 in which the transition state analogue dianion binds to the active protonated catalyst, Zn_2(**1**)(H_2O), but not to the ionized catalyst Zn_2(**1**)(HO^-). We concluded that Zn_2(**1**)(H_2O) is the active catalyst that stabilizes the transition state dianion and that it is converted to the inactive form Zn_2(**1**)(HO^-) when the pH is increased above pK_a = 7.8. Deprotonation of Zn_2(**1**)(H_2O) may inactivate the catalyst by changing the favorable displacement of the water ligand by the substrate phosphate monoanion to an unfavorable reaction for the displacement of the strongly basic hydroxide ion ligand.

A change in solvent from H_2O to D_2O causes an increase from 7.8 to 8.4 in the pK_a of the zinc-bound water at Zn_2(**1**)(L_2O) (Scheme 2), but has little effect on the reactivity of

SCHEME 5

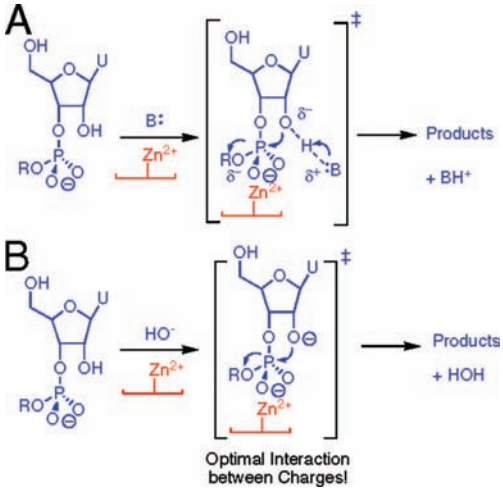

Zn_2(**1**)(L_2O) toward cleavage of UpPNP.[12] Therefore, there is no primary kinetic solvent deuterium isotope effect on the cleavage reaction that results from movement of a hydron in the rate-determining transition state,[12] such as occurs in reactions where there is concerted general base catalysis (GBC, Scheme 5A). We concluded that the phosphate diester cleavage reaction follows the specific-base-catalyzed (SBC) pathway shown in Scheme 5B.

We have proposed that the SBC pathway is observed for catalysis by these metal ion complexes because of the dominant role played by electrostatics in stabilization of the transition state for cleavage of RNA analogues by interactions with the metal ion complex catalyst (Scheme 5B).[12] In other words, that the "covalent"-type stabilization *gained* by placing the Brønsted base at the transition state for the GBC reaction (Scheme 5A) is smaller than the electrostatic stabilization *lost* upon partial neutralization of negative charge at the now partly protonated O-2.

Structure–Reactivity Effects

We next used the above kinetic protocols to examine the effect of systematic changes in the metal cation, ligand, and substrate structure on the transition state binding energy $\Delta G_S^{\ddagger}$ (Scheme 3) for reactions catalyzed by free metal ions and by metal ion complexes.

Ligand Effects. Chart 1 shows transition state binding energies ($\Delta G_S^{\ddagger}$, Scheme 3) for catalysis of the cleavage of HpPNP by several mononuclear Zn^{2+} complexes and by hydrated Zn^{2+}.[18] By comparison, a value of $\Delta G_S^{\ddagger} = -3.3$ kcal/mol was determined for Zn^{2+}-catalyzed deprotonation of acetone,[25] where Zn^{2+} interacts with a monoanionic rather than a dianionic transition state. A value of $\Delta G_S^{\ddagger} = -6.1$ kcal/mol was determined for Zn^{2+}-catalyzed aldose–ketose

CHART 1

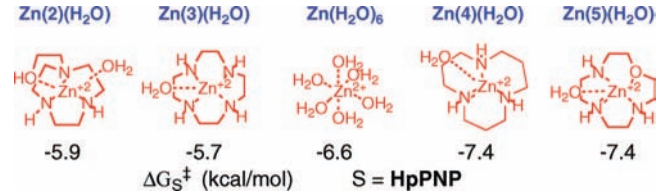

isomerization of trioses, where there is additional stabilization of the transition state from a *chelate* effect (Scheme 6).[26]

SCHEME 6

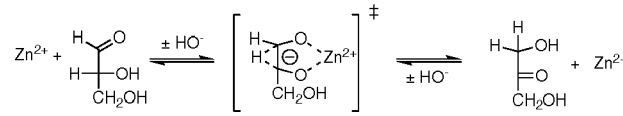

Zn^{2+} alone is a good catalyst of the cleavage of HpPNP (Chart 1). However, it is not possible to obtain large rate constants for this catalyzed cleavage at high pH, because of the sparing solubility of hydrated Zn^{2+}. Ligands **2**–**5** strongly enhance catalysis by increasing the total concentration of soluble metal cation. The small variation in $\Delta G_S^{\ddagger}$ across Chart 1 suggests a similar origin for the transition state stabilization, which we propose is mainly stabilizing electrostatic interactions between the metal cation and transition state dianion.[18]

Chart 1 shows that macrocycle ligands either increase or decrease the catalytic activity compared with the case where there is no ligand but that the effect on $\Delta G_S^{\ddagger}$ is no more than 1 kcal/mol. The formation of Zn^{2+} complexes has the effect of shifting positive charge from Zn^{2+} to the electron-donor ligand atom so that the weakest complexes will tend to show the highest charge density at Zn^{2+}. The complexes of Zn^{2+} to macrocycles **4** and **5** are substantially weaker than the complexes to **2** and **3**, but the weakly bound Zn^{2+} at the former complexes shows the greater catalytic activity (Chart 1).[18] The higher activity of Zn(**4**)(H_2O) and Zn(**5**)(H_2O) may be due to the larger positive charge density at the more weakly coordinated Zn^{2+}, and the resulting enhancement of stabilization from electrostatic interactions with the dianionic transition state.[18]

Cation Effects. The second-order rate constants for cleavage of HpPNP catalyzed by Cu_2(**1**)(H_2O) (Chart 2) are much smaller than those for catalysis by Zn_2(**1**)(H_2O) under the same conditions and are invariant between pH 7 and 10.[14] The X-ray crystal structure for Cu_2(**1**)(H_2O) shows a bridging alkoxide linker and a Cu(II)–Cu(II) distance of 3.58 Å,[27] similar to that observed in the crystal structure for Zn_2(**1**)(H_2O).[10] The structure for Zn_2(**1**)(H_2O) shows one hexacoordinated and one pentacoordinated Zn(II),[10] while the structure for Cu_2(**1**)(H_2O) shows two pentacoordinated

CHART 2

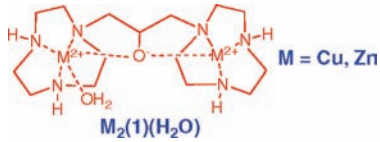

Cu(II).[27] We proposed that the coordination site missing from Cu_2(**1**)(H_2O) is essential for the efficient binding and catalysis of the reaction of HpPNP.

The larger absolute transition state binding energy of $\Delta G_S^{\ddagger}$ = 9.8 kcal/mol for cleavage of HpPNP catalyzed by Eu(III) (mainly $[Eu(OH_2)_9]^{3+}$)[19] in water than for cleavage catalyzed by hydrated Zn^{2+} in water ($\Delta G_S^{\ddagger}$ = 6.6 kcal/mol, Chart 1)[18] is probably due to the stronger stabilizing electrostatic interaction of a trication than of a dication with the transition state dianion. Chart 3 gives the values of $\Delta G_S^{\ddagger}$ for catalysis of cleavage of HpPNP by mononuclear Eu(III) complexes of **6**[16] and **7**,[19] and for a dinuclear complex that forms by spontaneous dimerization of **[Eu(6)(OH$_2$)$_2$]**$^+$ at pH ≥ 7.5.[16]

CHART 3

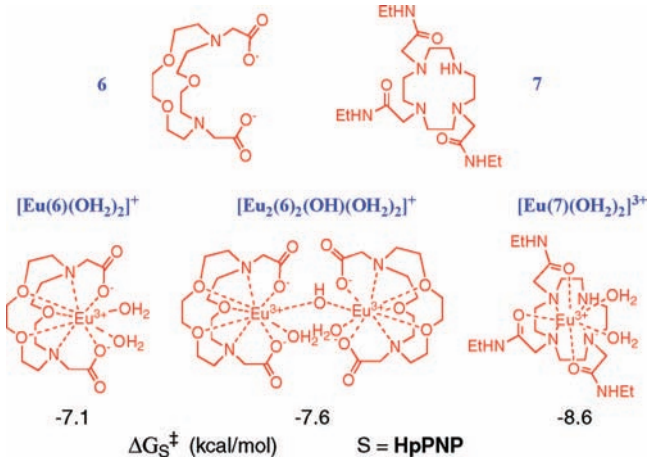

The absolute value of $\Delta G_S^{\ddagger}$ = 8.6 kcal/mol for catalysis by $[Eu(\mathbf{7})(OH_2)_2]^{3+}$ is only 1.2 kcal/mol larger than that observed for the most active mononuclear Zn(II) catalysts (Chart 1). Apparently, the larger number of donor groups to Eu(III) at $[Eu(\mathbf{7})(OH_2)_2]^{3+}$ compared with mononuclear Zn(II) catalysts act to attenuate the 3.2 kcal/mol larger transition state stabilization that is observed for catalysis by Eu(III) when all the ligands are water. The 1.5 kcal/mol larger absolute value of $\Delta G_S^{\ddagger}$ for $[Eu(\mathbf{7})(OH_2)_2]^{3+}$ than for $[Eu(\mathbf{6})(OH_2)_2]^{+}$ shows that there is a small increase in the catalytic efficiency with increasing total positive charge at the catalyst available to interact with the transition state dianion. Finally, the similar transition state binding energies for catalysis by $[Eu(\mathbf{6})(OH_2)_2]^{+}$ and $[Eu_2(\mathbf{6})_2(OH)(OH_2)_2]^{+}$ provide evidence that the two metal ions in the dimeric complex operate independently in catalyzing the cleavage of HpPNP.

Specificity. There are significant differences in the rate accelerations for the Zn_2(**1**)(H_2O)-catalyzed cleavage of RNA analogues and a dinucleoside monophosphate that reflect the different specificities of the dinuclear complex Zn_2(**1**)(H_2O) for transition state binding (Chart 4).[10,11,17,20] The binding "site" at this catalyst has not been characterized; however, it should not show strong shape complementarity to any of these substrates. We proposed other origins for the range of transition state binding energies shown in Chart 4.

CHART 4

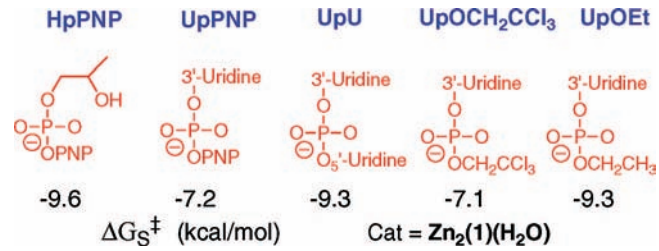

(1) The difference between $\Delta G_S^{\ddagger}$ = −9.6 and −7.2 kcal/mol for catalysis of cleavage of HpPNP, a minimal substrate, and of the more bulky substrate UpPNP, respectively, suggests that close approach of the phosphate diester to the metal cations is required for effective catalysis and that there is steric hindrance to the approach of the larger substrate UpPNP to Zn_2(**1**)(H_2O).[11]

(2) The difference between $\Delta G_S^{\ddagger}$ = −9.3 and −7.1 kcal/mol for catalysis of cleavage of UpOEt and $UpOCH_2CCl_3$, respectively, is a consequence of the different Brønsted parameters β_{lg} = −1.28 and −0.72 for the specific-base-catalyzed and Zn_2(**1**)(H_2O)-catalyzed cleavage reactions.[17,28] This corresponds to the neutralization of an effective transition state charge of ca. 0.56 units by interactions between the catalyst and the leaving group anion.[29] These data show that there is stabilization of the transition state for cleavage of UpOEt from interaction of the cationic catalyst with both the reacting phosphate core and the strongly basic alkoxy leaving group.

(3) The difference between $\Delta G_S^{\ddagger}$ = −9.3 and −7.2 kcal/mol for catalysis of cleavage of UpU and UpPNP, respectively, is due partly or entirely to transition state stabilization by interaction of the catalyst with the strongly basic alkoxy leaving group at UpU. There may also be a weak nonspecific interaction between the catalyst and the second pyrimidine base at UpU.[20]

Lessons from Studies on Small Molecule Catalysis

The high catalytic activity of Zn_2(**1**)(H_2O) arises from strong stabilizing binding interactions ($\Delta G_S^{\ddagger}$, Scheme 3) between the dianionic transition state and the densely charged cationic core of Zn_2(**1**)(H_2O).[10] No concerted general base catalysis of phosphate diester cleavage is observed, presumably because anything gained from such catalysis is offset by an even larger reduction in the electrostatic stabilization of the transition state (Scheme 5).

A distinguishing feature of these metal ion complex-catalyzed reactions is their large discrimination between the binding of the substrate phosphate diester monoanion (weak) and of the oxyphosphorane-like transition state dianion[30] and the methyl phosphate dianion transition state analogue (strong).[23] These results provide evidence that transition state stabilization by mononuclear and dinuclear metal ion complexes is due largely to electrostatic interactions, which are optimal for the dianionic transition state and transition state analogue. In other words, good catalysis of the cleavage of phosphate diesters in water has been obtained relatively easily because of the intrinsically strong stabilizing interactions between densely charged metals and phosphate dianions. The total transition state binding energy $\Delta G_S^{\ddagger}$ can be modified by interactions between the metal ion and its ligands, but these effects are small in comparison with the transition state stabilization observed for catalysis by free metal ions, where the ligands are water (Chart 1).

Enzyme Catalysis

A major difference between small molecule and enzyme catalysts is that the latter have evolved mechanisms for utilization of the binding interactions between the protein and nonreacting portions of the substrate in stabilization of the transition state for the catalyzed reaction.[2] The transition state binding energies of up to −10 kcal/mol observed for catalysis of the cleavage of phosphate diesters are due mainly to electrostatic interactions between the catalyst and the phosphate group, which is the reaction center. We have observed even larger transition state stabilizations of ca. 12 kcal/mol from utilization of the binding energy between enzyme catalysts and the *nonreacting* phosphodianion group of substrates for enzyme-catalyzed proton transfer, hydride transfer, and decarboxylation reactions.[31−33]

Reactions of Triosephosphates

Triosephosphate isomerase (TIM) is a prototypical catalyst of proton transfer at carbon (Chart 5). This enzyme catalyzes the stereospecific 1,2-hydrogen shift at (*R*)-glyceraldehyde 3-phosphate (GAP) to give dihydroxyacetone phosphate (DHAP). A single base (Glu-165) catalyzes suprafacial proton transfer through a *cis*-enediol(ate) intermediate.[34] The ratio of second-order rate constants $(k_{cat}/K_m)_{GAP}/(k_{cat}/K_m)_{GA} = (2.4 \times 10^8\ M^{-1}\ s^{-1})/(0.34\ M^{-1}\ s^{-1}) = 7 \times 10^8$ for the TIM-catalyzed isomerization of GAP and of (*R*)-glyceraldehyde shows that binding interactions between the enzyme and the phosphodianion group of GAP provide ≥12 kcal/mol of transition state stabilization.[35] This may account for all but 2 kcal/mol of the transition state stabilization for TIM-catalyzed isomerization of GAP.[35,36]

CHART 5

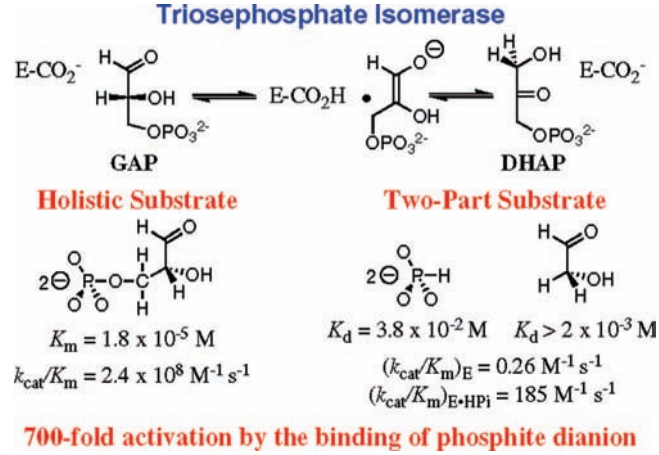

The value of $(k_{cat}/K_m)_{Gly} = 0.26\ M^{-1}\ s^{-1}$ for TIM-catalyzed exchange of deuterium from solvent D_2O into the truncated substrate glycolaldehyde is similar to $(k_{cat}/K_m)_{GA} = 0.34\ M^{-1}\ s^{-1}$ for isomerization of (*R*)-glyceraldehyde.[31] The deuterium exchange reaction of glycolaldehyde is strongly activated by addition of the second substrate "piece" phosphite dianion, HPO_3^{2-}. The data give $(k_{cat}/K_m)_{E\cdot HPi} = 185\ M^{-1}\ s^{-1}$ for turnover of glycolaldehyde by TIM that is saturated with phosphite dianion, so binding of phosphite dianion to TIM results in a 700-fold rate acceleration of proton transfer from carbon. The two substrate pieces, glycolaldehyde and HPO_3^{2-}, each bind weakly to TIM, and there is a large "chelate" effect for binding of the whole substrate GAP (Chart 5).[31,37] The binding of HPO_3^{2-} to free TIM (K_d = 38 mM) is 700-fold weaker than its binding to the fleeting TIM·transition state complex ($K_d^{\ddagger}$ = 53 μM, Scheme 7). This corresponds to an intrinsic phosphite dianion binding energy of −5.8 kcal/mol (Scheme 7).[31]

The proton transfer reaction catalyzed by TIM occurs in an active site at which the substrate is sequestered from solvent.[38,39] We proposed a model for catalysis by TIM in

SCHEME 7

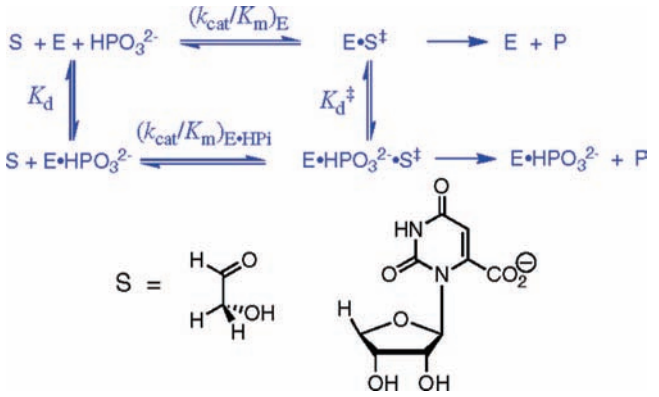

which part of the total intrinsic binding energy of the phosphodianion group of substrate is utilized to drive a protein conformational change that sequesters the substrate at an active site with an apparent dielectric constant substantially lower than that of solvent and with the catalytic groups optimally organized to stabilize the transition state for deprotonation of α-carbonyl carbon.[31,40]

SCHEME 8

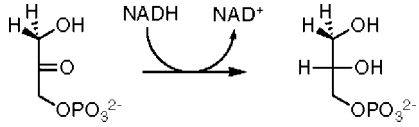

The whole substrate DHAP is reduced by NADH to give L-glycerol 3-phosphate in a reaction catalyzed by α-glycerol phosphate dehydrogenase (Scheme 8).[41] The ratio $(k_{cat}/K_m)_{DHAP}/(k_{cat}/K_m)_{Gly} = (1 \times 10^6\ M^{-1}\ s^{-1})/(0.009\ M^{-1}\ s^{-1}) = 1.1 \times 10^8$ for rabbit muscle α-glycerol phosphate dehydrogenase-catalyzed reduction of DHAP and glycolaldehyde gives an intrinsic phosphate binding energy of −11 kcal/mol, which is similar to that for TIM.[33] We find that phosphite dianion is also a powerful activator of enzyme-catalyzed reduction of the truncated neutral substrate glycolaldehyde by NADH.[33] X-ray crystallographic analysis of human α-glycerol phosphate dehydrogenase provides evidence that the phosphate binding energy of the substrate is used to *drive* the closure of a loop over the substrate.[41]

Orotidine 5′-Monophosphate Decarboxylase (OMPDC)

OMPDC is a remarkable enzyme that effects an enormous 10^{17}-fold acceleration of the chemically very difficult decarboxylation of orotidine 5′-monophosphate (OMP, Chart 6) to give uridine 5′-monophosphate (UMP).[42] The enzymatic[43] and nonenzymatic[44] decarboxylation reactions proceed through the vinyl carbanion intermediates. Comparison of the X-ray crystal structures of free yeast OMPDC and that complexed with the transition state analogue 6-hydroxyuridine 5′-monophosphate shows that ligand binding results in a large motion to "close" the active site with the formation of numerous protein–ligand contacts, including five hydrogen bonds to the phosphodianion group.[45] The phosphodianion at OMP, or at any phosphorylated enzymatic substrate, may simply "anchor" the substrate to the enzyme, or the enzyme conformational change effected by the small remote group may directly assist in the creation of an active site that provides optimal transition state stabilization.

CHART 6

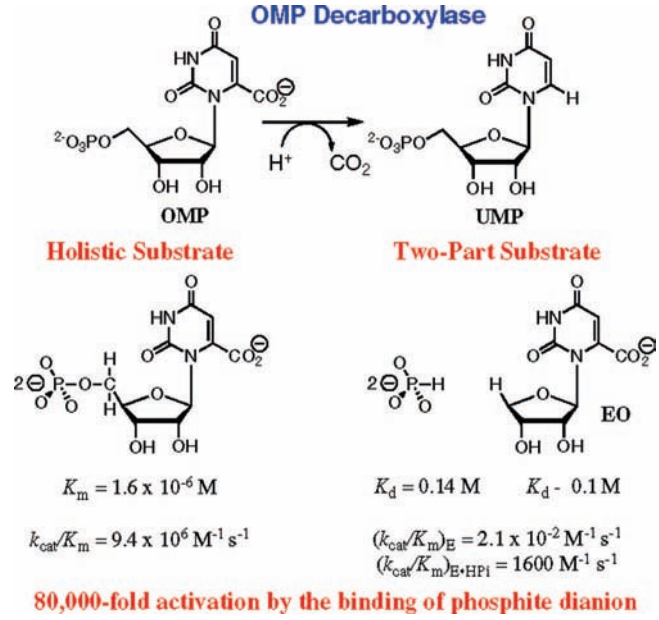

The intrinsic binding energy of the phosphodianion group of OMP, calculated from the ratio of second-order rate constants k_{cat}/K_m for the OMPDC-catalyzed reactions of OMP ($9.4 \times 10^6\ M^{-1}\ s^{-1}$)[46] and the truncated substrate 1-(β-D-erythrofuranosyl)orotic acid (EO, $2.1 \times 10^{-2}\ M^{-1}\ s^{-1}$)[32] is −12 kcal/mol (Chart 6). The weak binding of the EO ($K_d \approx 0.1$ M) and phosphite dianion ($K_d = 0.14$ M) pieces to OMPDC is striking in view of the tight binding of the whole substrate OMP ($K_m = 1.6\ \mu$M).[37,46] Decarboxylation of EO is strongly activated by phosphite dianion, with $(k_{cat}/K_m)_{E\cdot HPi} = 1600\ M^{-1}\ s^{-1}$ for turnover of EO by OMPDC that is saturated with HPO_3^{2-}, so the binding of this dianion to OMPDC results in an 80000-fold acceleration of decarboxylation.[32] The binding of HPO_3^{2-} to OMPDC ($K_d = 0.14$ M) must also be 80000-fold weaker than its binding to the fleeting complex of OMPDC with EO in the transition state ($K_d^{\ddagger} = 1.8\ \mu$M, Scheme 7). The total intrinsic binding energy of HPO_3^{2-} at the transition state complex is therefore −7.8 kcal/mol. This is divided into the small −1.2

kcal/mol binding energy observed in the ground-state complex and an additional −6.6 kcal/mol interaction that develops on proceeding to the transition state for enzyme-catalyzed decarboxylation of EO.[2,32]

The Pauling Paradigm

Our studies have shown that the interactions between nonreacting phosphodianion fragments of substrate and the protein provide an 11−12 kcal/mol stabilization of the transition states for proton transfer, hydride transfer, and decarboxylation reactions. Therefore, enzymes that catalyze the reactions of small phosphorylated substrates such as GAP and DHAP have a potential transition state binding energy of −12 kcal/mol. The medium-sized phosphorylated substrate OMP interacts with OMPDC via its phosphodianion, ribose sugar ring, and nucleic acid base portions and exhibits a transition state binding energy far in excess of −15 kcal/mol that was proposed as the limit on noncovalent enzyme catalysis.[3,42]

Pyridoxal 5′-phosphate (PLP) provides impressive covalent catalysis of the deprotonation of α-amino acids to form α-amino carbanions.[47] However, the large rate acceleration for proton transfer obtained by recruitment of this cofactor can be also obtained by protein catalysts, such as proline racemase. This enzyme provides a 19 kcal/mol stabilization of the transition state for deprotonation of enzyme-bound proline by interaction with the protein catalyst.[48] Our proposal that "pure protein catalysis" of deprotonation of amino acids results from the binding of the amino acid substrate at a nonpolar active site that favors formation of a carbanion zwitterion[49,50] has been supported by X-ray crystallographic and computational studies.[51,52] We are generally skeptical of arguments that cofactors such as PLP have evolved to do what is impossible for protein catalysts, because of the great diversity of protein-catalyzed reactions. On the other hand, cofactor catalysis is often simpler and more general than protein catalysis, and these factors favor the recruitment of cofactors in enzymatic catalysis.

We acknowledge the NSF (Grant CHE0415356) and the NIH (Grant GM39754) for support of our work, and we thank our co-workers named in the references for their many contributions to our research.

BIOGRAPHICAL INFORMATION

Janet R. Morrow received a B.S. degree in chemistry from the University of California, Santa Barbara, and her Ph.D. degree in chemistry (1985) from the University of North Carolina, Chapel Hill. She is currently Professor of Chemistry at the University at Buffalo, SUNY.

Tina L. Amyes received B.A. and M.A. degrees in natural sciences and her Ph.D. degree in chemistry (1986) from the University of Cambridge (England). She is currently an Adjunct Associate Professor at the University at Buffalo, SUNY.

John P. Richard received a B.S. degree in biochemistry and his Ph.D. degree in chemistry (1979) from The Ohio State University. He is currently Professor of Chemistry at the University at Buffalo, SUNY.

FOOTNOTES

*E-mail: jrichard@chem.buffalo.edu.

REFERENCES

1 Pauling, L. The nature of forces between large molecules of biological interest. *Nature* **1948**, *161*, 707–709.
2 Jencks, W. P. Binding energy, specificity and enzymic catalysis: The circe effect. *Adv. Enzymol. Relat. Areas Mol. Biol.* **1975**, *43*, 219–410.
3 Zhang, X.; Houk, K. N. Why enzymes are proficient catalysts: Beyond the Pauling paradigm. *Acc. Chem. Res.* **2005**, *38*, 379–385.
4 Morrow, J.; Iranzo, O. Synthetic metallonucleases for RNA cleavage. *Curr. Opin. Chem. Biol.* **2004**, *8*, 192–200.
5 Williams, N. H.; Takashi, B.; Wall, M.; Chin, J. Structure and nuclease activity of simple dinuclear metal complexes: quantitative dissection of the role of metal ions. *Acc. Chem. Res.* **1999**, *32*, 485–493.
6 Blasko, A.; Bruice, T. C. Recent studies of nucleophilic, general-acid and metal ion catalysis of phosphate diester hydrolysis. *Acc. Chem. Res.* **1999**, *32*, 475–484.
7 Chin, K. O. A.; Morrow, J. R. RNA cleavage and phosphate diester transesterification by encapsulated lanthanide ions: Traversing the lanthanide series with lanthanum(III), europium(III), and lutetium(III) complexes of 1,4,7,10-tetrakis(2-hydroxyalkyl)-1,4,7,10-tetraazacyclododecane. *Inorg. Chem.* **1994**, *33*, 5036–5041.
8 Morrow, J. R.; Buttrey, L. A.; Shelton, V. M.; Berback, K. A. Efficient catalytic cleavage of RNA by lanthanide(III) macrocyclic complexes: Toward synthetic nucleases for in vivo applications. *J. Am. Chem. Soc.* **1992**, *114*, 1903–1905.
9 Baker, B. F.; Khalili, H.; Wei, N.; Morrow, J. R. Cleavage of the 5′ cap structure of *m*RNA by a europium(III) macrocyclic complex with pendant alcohol group. *J. Am. Chem. Soc.* **1997**, *119*, 8749–8755.
10 Iranzo, O.; Kovalevsky, A. Y.; Morrow, J. R.; Richard, J. P. Physical and kinetic analysis of the cooperative role of metal ions in catalysis of phosphodiester cleavage by a dinuclear Zn(II) complex. *J. Am. Chem. Soc.* **2003**, *125*, 1988–1993.
11 Yang, M.-Y.; Richard, J. P.; Morrow, J. R. Substrate specificity for catalysis of phosphodiester cleavage by a dinuclear Zn(II) complex. *Chem. Commun.* **2003**, 2832–2833.
12 Yang, M.-Y.; Iranzo, O.; Richard, J. P.; Morrow, J. R. Solvent deuterium isotope effects on phosphodiester cleavage catalyzed by an extraordinarily active Zn(II) complex. *J. Am. Chem. Soc.* **2005**, *127*, 1064–1065.
13 Feng, G.; Mareque-Rivas, J. C.; Williams, N. H. Comparing a mononuclear Zn(II) complex with hydrogen bond donors with a dinuclear Zn(II) complex for catalysing phosphate ester cleavage. *Chem. Commun.* **2006**, 1845–1847.
14 Iranzo, O.; Richard, J. P.; Morrow, J. R. Structure−activity studies on the cleavage of an RNA analogue by a potent dinuclear metal ion catalyst. The effect of changing the metal ion. *Inorg. Chem.* **2004**, *43*, 1743–1750.
15 Iranzo, O.; Elmer, T.; Richard, J. P.; Morrow, J. R. Cooperativity between metal ions in the cleavage of phosphate diesters and RNA by dinuclear Zn(II) catalysts. *Inorg. Chem.* **2003**, *42*, 7737–7746.
16 Farquhar, E.; Richard, J. P.; Morrow, J. R. Formation and stability of mononuclear and dinuclear Eu(III) complexes and their catalytic reactivity toward cleavage of an RNA analogue. *Inorg. Chem.* **2007**, *46*, 7169–7177.
17 Yang, M.-Y. Ph.D. Thesis, University at Buffalo, 2007.
18 Mathews, R. A.; Rossiter, C. S.; Morrow, J. R.; Richard, J. P. A minimalist approach to understanding the efficiency of mononuclear Zn(II) complexes as catalysts of cleavage of an RNA analogue. *Dalton Trans.* **2007**, 3804–3811.
19 Nwe, K.; Richard, J. P.; Morrow, J. R. Direct excitation luminescence spectroscopy of Eu(III) complexes of 1,4,7-tris(carbamoylmethyl)-1,4,7,10- tetraazacyclododecane derivatives and kinetic studies of their catalytic cleavage of an RNA analog. *Dalton Trans.* **2007**, 5171–5178.
20 O'Donoghue, A.; Pyun, S. Y.; Yang, M.-Y.; Morrow, J. R.; Richard, J. P. Substrate specificity of an active dinuclear complex for cleavage of RNA analogues and a dinucleoside. *J. Am. Chem. Soc.* **2006**, *128*, 1615–1621.

21 Feng, G.; Mareque-Rivas, J. C.; Torres Martin de Rossales, R.; Williams, N. H. A highly reactive mononuclear Zn(II) complex for phosphodiester cleavage. *J. Am. Chem. Soc.* **2005**, *127*, 13470–13471.

22 Neverov, A. A.; Lu, Z. L.; Maxwell, C. I.; Mohamed, M. F.; White, C. J.; Tsang, J. S. W.; Brown, R. S. Combination of a dinuclear Zn^{2+} complex and a medium effect exerts a 10^{12}-fold rate enhancement of cleavage of an RNA and DNA model system. *J. Am. Chem. Soc.* **2006**, *128*, 16398–16405.

23 Yang, M.-Y.; Morrow, J. R.; Richard, J. P. A transition state analog for phosphate diester cleavage catalyzed by a small enzyme-like metal ion complex. *Bioorg. Chem.* **2007**, *35*, 366–374.

24 Wolfenden, R. Transition state analogues for enzyme catalysis. *Nature* **1969**, *223*, 704–705.

25 Crugeiras, J.; Richard, J. P. A comparison of the electrophilic reactivities of Zn^{2+} and acetic acid as catalysts of enolization: imperatives for enzymatic catalysis of proton transfer at carbon. *J. Am. Chem. Soc.* **2004**, *126*, 5164–5173.

26 Nagorski, R. W.; Richard, J. P. Mechanistic imperatives for aldose-ketose isomerization in water: specific-, general base- and metal ion-catalyzed isomerization of glyceraldehyde with proton and hydride transfer. *J. Am. Chem. Soc.* **2001**, *123*, 794–802.

27 Fry, F. H.; Moubaraki, B.; Murray, K. S.; Spiccia, L.; Warren, M.; Skelton, B. W.; White, A. H. Asymmetry in endogenously bridged binuclear copper(II) and zinc(II) complexes formed by 1,2-bis[1,4,7-triazacyclonon-1-yl]-propan-2-ol. *Dalton Trans.* **2003**, 866–871.

28 Kosonen, M.; Youseti-Salakdeh, E.; Stromberg, R.; Lönnberg, H. Mutual isomerization of uridine 2′- and 3′-alkylphosphates and cleavage to a 2′,3′-cyclic phosphate: the effect of the alkyl group on the hydronium- and hydroxide-ion-catalyzed reactions. *J. Chem. Soc., Perkin Trans. 2* **1997**, 2661–2666.

29 Williams, A. Electronic charge and transition state structure in solution. *Adv. Phys. Org. Chem.* **1992**, *27*, 1–55.

30 Perreault, D. M.; Anslyn, E. V. Unifying the current data on the mechanism of cleavage-transesterification of RNA. *Angew. Chem., Int. Ed. Engl.* **1997**, *36*, 432–450.

31 Amyes, T. L.; Richard, J. P. Enzymatic catalysis of proton transfer at carbon: Activation of triosephosphate isomerase by phosphite dianion. *Biochemistry* **2007**, *46*, 5841–5854.

32 Amyes, T. L.; Richard, J. P.; Tait, J. J. Activation of orotidine 5′-monophosphate decarboxylase by phosphite dianion: the whole substrate is the sum of two parts. *J. Am. Chem. Soc.* **2005**, *127*, 15708–15709.

33 Tsang, W.-Y.; Amyes, T. L.; Richard, J. P. A Substrate in Pieces: Allosteric Activation of Glycerol 3-Phosphate Dehydrogenase (NAD^+) by Phosphite Dianon, *Biochemistry*, submitted for publication.

34 Knowles, J. R.; Albery, W. J. Perfection in enzyme catalysis: The energetics of triosephosphate isomerase. *Acc. Chem. Res.* **1977**, *10*, 105–111.

35 Amyes, T. L.; O'Donoghue, A. C.; Richard, J. P. Contribution of phosphate intrinsic binding energy to the enzymatic rate acceleration for triosephosphate isomerase. *J. Am. Chem. Soc.* **2001**, *123*, 11325–11326.

36 Richard, J. P. Acid-base catalysis of the elimination and isomerization reactions of triose phosphates. *J. Am. Chem. Soc.* **1984**, *106*, 4926–4936.

37 Jencks, W. P. On the attribution and additivity of binding energies. *Proc. Natl. Acad. Sci. U.S.A.* **1981**, *78*, 4046–4050.

38 O'Donoghue, A. C.; Amyes, T. L.; Richard, J. P. Hydron transfer catalyzed by triosephosphate isomerase. Products of isomerization of (*R*)-glyceraldehyde 3-phosphate in D_2O. *Biochemistry* **2005**, *44*, 2610–2621.

39 O'Donoghue, A. C.; Amyes, T. L.; Richard, J. P. Hydron transfer catalyzed by triosephosphate isomerase. Products of isomerization of dihydroxyacetone phosphate in D_2O. *Biochemistry* **2005**, *44*, 2622–2631.

40 Sampson, N. S.; Knowles, J. R. Segmental motion in catalysis: Investigation of a hydrogen bond critical for loop closure in the reaction of triosephosphate isomerase. *Biochemistry* **1992**, *31*, 8488–8494.

41 Ou, X.; Ji, C.; Han, X.; Zhao, X.; Li, X.; Mao, Y.; Wong, L.-L.; Bartlam, M.; Rao, Z. Crystal structure of human glycerol 3-phosphate dehydrogenase (GPDI). *J. Mol. Biol.* **2006**, *357*, 858–869.

42 Radzicka, A.; Wolfenden, R. A proficient enzyme. *Science* **1995**, *267*, 90–93.

43 Toth, K.; Amyes, T. L.; Wood, B. M.; Chan, K.; Gerlt, J. A.; Richard, J. P. Product deuterium isotope effect for orotidine 5′-monophosphate decarboxylase: Evidence for the existence of a short-lived carbanion intermediate. *J. Am. Chem. Soc.* **2007**, *129*, 12946–12947.

44 Sievers, A.; Wolfenden, R. Equilibrium of formation of the 6-carbanion of UMP, a potential intermediate in the action of OMP decarboxylase. *J. Am. Chem. Soc.* **2002**, *124*, 13986–13987.

45 Miller, B. G.; Hassell, A. M.; Wolfenden, R.; Milburn, M. V.; Short, S. A. Anatomy of a proficient enzyme: The structure of orotidine 5′-monophosphate decarboxylase in the presence and absence of a potential transition state analog. *Proc. Natl. Acad. Sci. U.S.A.* **2000**, *97*, 2011–2016.

46 Porter, D. J. T.; Short, S. A. Yeast orotidine-5′-phosphate decarboxylase: Steady-state and pre-steady-state analysis of the kinetic mechanism of substrate decarboxylation. *Biochemistry* **2000**, *39*, 11788–11800.

47 Toth, K.; Richard, J. P. Covalent catalysis by pyridoxal: Evaluation of the effect of the cofactor on the carbon acidity of glycine. *J. Am. Chem. Soc.* **2007**, *129*, 3013–3021.

48 Williams, G.; Maziarz, E. P.; Amyes, T. L.; Wood, T. D.; Richard, J. P. Formation and stability of the enolates of N-protonated proline methyl ester and proline zwitterion in aqueous solution: a nonenzymatic model for the first step in the racemization of proline catalyzed by proline racemase. *Biochemistry* **2003**, *42*, 8354–8361.

49 Rios, A.; Amyes, T. L.; Richard, J. P. Formation and stability of organic zwitterions in aqueous solution: Enolates of the amino acid glycine and its derivatives. *J. Am. Chem. Soc.* **2000**, *122*, 9373–9385.

50 Richard, J. P.; Amyes, T. L. On the importance of being zwitterionic: Enzymic catalysis of decarboxylation and deprotonation of cationic carbon. *Bioorg. Chem.* **2004**, *32*, 354–366.

51 Puig, E.; Garcia-Viloca, M.; Gonzalez-Lafont, A.; Lluch, J. M. On the ionization state of the substrate in the active site of glutamate racemase. A QM/MM study about the importance of being zwitterionic. *J. Phys. Chem. A* **2006**, *110*, 717–725.

52 Pillai, B.; Cherney, M. M.; Diaper, C. M.; Sutherland, A.; Blanchard, J. S.; Vereras, J. C.; James, M. N. G. Structural insights into stereochemical inversion by diaminopimilate epimerase: an antibacterial drug target. *Proc. Natl. Acad. Sci. U.S.A.* **2006**, *103*, 8668–8673.